Osmotic blood-brain barrier disruption: CT and radionuclide imaging.

S Roman-Goldstein, D A Clunie, J Stevens, R Hogan, J Monard, F Ramsey and E A Neuwelt

AJNR Am J Neuroradiol 1994, 15 (3) 581-590
http://www.ajnr.org/content/15/3/581

Osmotic Blood-Brain Barrier Disruption: CT and Radionuclide Imaging

Simon Roman-Goldstein, David A. Clunie, Jeffrey Stevens, Raymond Hogan, John Monard, Fred Ramsey, and Edward A. Neuwelt

PURPOSE: To compare CT and radionuclide imaging of osmotic blood-brain barrier disruption. To develop a quantitative method for imaging osmotic blood-brain barrier disruption and to see if iopamidol could be safely given intravenously in conjunction with blood-brain barrier disruption. **METHODS:** Forty-five blood-brain barrier disruption procedures were imaged with CT and radionuclide scans. The scans were evaluated with visual and quantitative scales. Patients were observed for adverse effects after blood-brain barrier disruption. **RESULTS:** There was a 4% rate of seizures in this study. There was good agreement between visual CT and radionuclide grading systems. Quantitative methods to grade disruption did not add useful information to visual interpretations. **CONCLUSIONS:** Nonionic iodine-based contrast medium has a lower incidence of seizures when injected intravenously in conjunction with osmotic blood-brain barrier disruption than ionic contrast material. Contrast-enhanced CT is the preferred method to image disruption because it has better spatial resolution than radionuclide techniques.

Index terms: Blood-brain barrier; Brain, computed tomography; Brain, radionuclide studies; Contrast media, nonionic; Computed tomography, comparative studies; Radionuclide imaging, comparative studies

AJNR Am J Neuroradiol 15:581–590, Mar 1994

Osmotic blood-brain barrier disruption, a procedure that increases drug delivery, with intra-arterial chemotherapy has been effective treatment for human brain tumors (1–3). Imaging the degree of disruption is an important component of this therapy; animal studies have shown correlation with the degree of disruption and methotrexate delivery to brain (4).

Initially blood-brain barrier disruption was imaged by injecting 150 mL of meglumine iothalamate (Conray 60, Mallinckrodt, St Louis) intravenously immediately after disruption and obtaining computed tomographic (CT) scans of the brain. This was associated with a 16% rate of seizure versus 8% when meglumine iothalamate was not injected (5). Since then, blood-brain barrier disruption has been imaged by injecting 740 mBq of technetium-99m-glucoheptonate immediately after blood-brain barrier disruption and obtaining radionuclide images 3 hours after blood-brain barrier disruption, but this method suffers from a lack of spatial resolution.

Prior canine studies have shown that unenhanced magnetic resonance (MR) with both T1-weighted and T2-weighted images is unable to image disruption (6, 7). In a canine model of osmotic blood-brain barrier disruption, gadopentetate dimeglumine (Magnevist, Berlex Imaging, Wayne, NJ) was associated with delayed seizures when injected intravenously (6). The results of these prior studies are why MR has not been used to image disruption in patients with brain tumors.

This study was done to see if a nonionic iodine contrast agent could be given intravenously in conjunction with osmotic blood-brain barrier disruption with less toxicity than ionic contrast. Next, visual analysis of CT and radionuclide images were compared to determine which method was superior for imaging blood-brain barrier disruption. Last, quantitative methods were applied

Received January 4, 1993; accepted pending revision February 9; revision received March 19.

This work was supported by a Veterans Administration Merit Review Grant and National Institutes of Health, Grant RO1 31770–10.

From the Oregon Health Sciences University (S.R.-G., D.A.C., J.S., R.H., J.M., E.A.N.), Portland; and Oregon State University, Department of Statistics (F.R.), Corvallis.

Address reprint requests to Edward A. Neuwelt, MD, Oregon Health Sciences University, Division of Neurology, L603, 3181 SW Sam Jackson Park Road, Portland, OR 97201-3098.

AJNR 15:581–590, Mar 1994 0195-6108/94/1503–0581

to CT and radionuclide images to determine whether numerical analysis added useful information to visual analysis of CT and radionuclide scans.

Patients and Methods

Performing Blood-Brain Barrier Disruption

Patients are referred to our institution for treatment with osmotic blood-brain barrier disruption and intraarterial chemotherapy as previously described (1, 2). The procedure is done under general anesthesia. A transfemoral approach is used to catheterize either an internal carotid artery or a vertebral artery. The catheter is placed at the C1–2 area for internal carotid artery injections and the C-6 level for vertebral artery injections. Warmed, filtered, 25% mannitol is then infused at a rate of 6 to 12 mL/sec for 30 seconds into the artery followed by the intraarterial administration of chemotherapy. The study period was from December 18, 1990 to March 31, 1991. During that time, 45 blood-brain barrier disruption procedures in 15 patients were obtained. Eleven disruptions were performed in the right internal carotid artery territory, 14 in the left internal carotid artery territory, and 20 in a vertebral artery territory. The patient characteristics are summarized in Table 1.

Imaging Disruption

Immediately after blood-brain barrier disruption 740 mBq of Tc-99m-glucoheptonate and 150 mL of Isovue 300 (iopamidol 61%, Squibb Diagnostics, New Brunswick, NJ) were administered intravenously. One half-hour after blood-brain barrier disruption, CT images were obtained on a 9800 CT scanner (General Electric, Milwaukee, Wis) with 5-mm-thick sections through the posterior fossa and 10-mm-thick sections through the remainder of the brain. Planar radionuclide images were obtained 3 hours after disruption with anterior, posterior, and vertex images acquired on a Maxicamera (General Electric) for internal carotid artery disruptions and posterior images for vertebral artery disruptions.

Visual CT Grading of Blood-Brain Barrier Disruption

Visual grading was done on CT and radionuclide scans by comparing the enhancement or activity in the disrupted territories with the nondisrupted territories. For internal carotid artery disruptions enhancement or activity in the anterior cerebral artery territory or middle cerebral artery territory ipsilateral to the disruption was compared with the contralateral anterior cerebral artery or middle cerebral artery territory. For posterior fossa disruptions the enhancement or activity in both cerebellar hemispheres, thalami, or posterior cerebral artery territories were compared with the anterior cerebral artery and middle cerebral artery territories. The overall grade of the disruption was the grade of the disrupted territory that showed the greatest increase in enhancement or activity similar to the convention used in animal studies (4). One neuroradiologist simultaneously performed the visual grading of disruption on both the CT and radionuclide images. The visual scales are summarized in Table 2.

Quantitative CT Grading of Blood-Brain Barrier Disruption

Quantitative imaging of blood-brain barrier disruption was also performed using the CT images. Hounsfield unit (HU) measurements were obtained in regions of interest in four anterior circulation territories defined as bilateral anterior cerebral artery territories (Fig 1) and middle cerebral artery territories (Fig 2), and then in six posterior circulation

TABLE 1: Patient characteristics/procedures

Patient	Sex	Age	Diagnosis	Disruptions			
				Total	RICA	LICA	VA
1	M	42	Gliomatosis cerebri	6	2	2	2
2	M	23	Glioblastoma multiforme	4	0	2	2
3	M	48	Primary central nervous system lymphoma	3	1	1	1
4	M	44	Glioblastoma multiforme	3	1	0	2
5	M	31	Glioblastoma multiforme	4	0	2	2
6	F	47	Carcinomatous meningitis from breast	4	2	1	1
7	M	34	Primary central nervous system lymphoma	3	1	1	1
8	M	29	Germinoma	2	0	0	2
9	M	31	Germinoma	3	1	1	1
10	F	18	Brain stem glioma	1	0	0	1
11	M	67	Primary central nervous system lymphoma	4	0	2	2
12	M	14	Germinoma	2	1	0	1
13	M	69	Primary central nervous system lymphoma	2	1	1	0
14	M	52	Glioblastoma multiforme	2	0	1	1
15	F	70	Primary central nervous system lymphoma	2	1	0	1
Totals				45	11	14	20

Note.—RICA indicates right internal carotid artery; LICA, left internal carotid artery; and VA, vertebral artery.

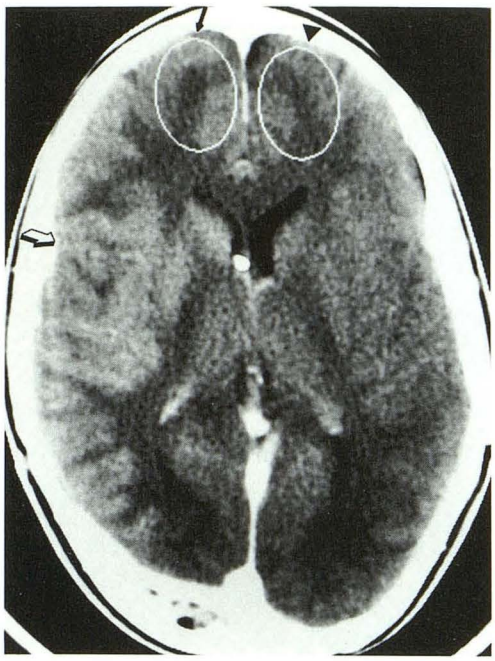

A

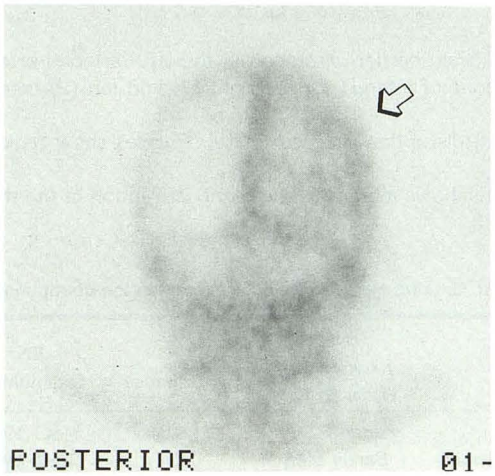

B

Fig. 1. *A*, Contrast-enhanced CT scan after an osmotic blood-brain barrier disruption in the right internal carotid artery on patient 12. This was a grade 2 (good) disruption in the right middle cerebral artery territory (*open arrow*). The *circles* show the territories for region of interest calculation by the left (*arrowhead*) and right (*arrow*) anterior cerebral artery distributions.

B, Posterior view of a radionuclide brain scan in the same patient on the same date showing a grade 2 (good) disruption in the right middle cerebral artery territory (*arrow*).

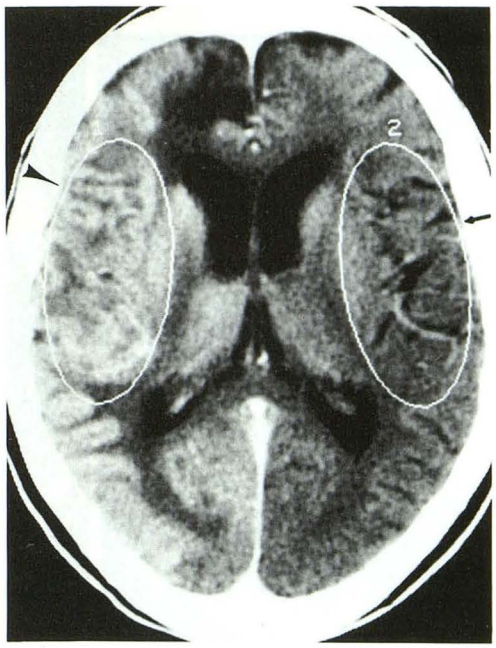

A

B

Fig. 2. *A*, CT scan after an osmotic blood-brain barrier disruption in the right internal carotid artery on patient 15 shows a grade 3 (excellent) disruption in the right middle cerebral artery territory (*arrowhead*). *Ellipses* indicate where regions of interest were drawn in the left (*arrow*) and right (*arrowhead*) middle cerebral artery distributions.

B, Posterior view of a radionuclide brain scan in the same patient on the same date showing a grade 3 (excellent) disruption in the right middle cerebral artery territory (*arrow*).

territories defined as the posterior cerebral artery territories, bilateral cerebellar hemispheres (Fig 3), and thalami (Fig 4). A statistician familiar with the visual grading system but blinded to the visual grades of each individual scan developed a quantitative grading system based on the median values and interquartile ranges of these data. For internal carotid artery disruptions, the anterior circulation grades were based on the difference in HU measurements between the disrupted and nondisrupted middle cerebral artery territories on a scale summarized in Table 2A. VA disruptions were graded based on the difference between the average HU in the posterior circulation territories and the average HU in the anterior circulation territories on a scale summarized in Table 2B.

Quantitative Radionuclide Grading of Blood-Brain Barrier Disruption

For analysis of the anterior circulation procedure, regions of interest in the anterior, posterior, and vertex views

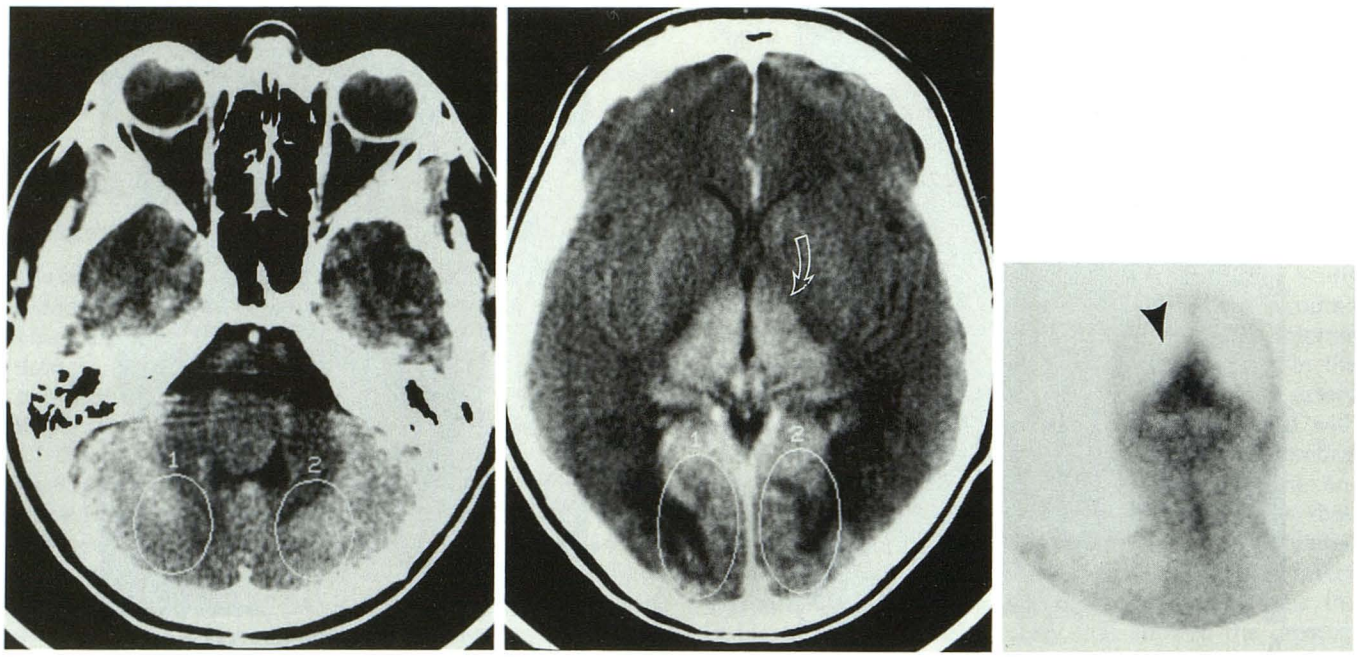

Fig. 3. *A*, Contrast-enhanced CT scan through the cerebellum after a blood-brain barrier disruption in the left vertebral artery on patient 10 shows no appreciable enhancement. *Ellipses* are an example of regions of interest for the right (*1*) and left (*2*) cerebellar hemispheres.

B, Image on the same scan as in *A* shows evidence of a grade 3 (excellent) disruption (*curved arrow*). *Ellipses* show regions of interest for the posterior cerebral artery distribution.

C, Posterior view of a radionuclide scan in the same patients on the same date shows a grade 3 (excellent) disruption in the thalami (*arrowhead*).

are drawn by hand with a light pen, covering territory supplied by the disrupted and nondisrupted internal carotid arteries. The ratio of mean counts per pixel for the disrupted versus nondisrupted side is obtained and averaged for all regions on all views. Internal carotid artery disruptions are graded on a scale summarized in Table 2A.

For analysis of posterior circulation disruptions, the posterior view radionuclide scan is used with regions of interest drawn over each cerebellar hemisphere, over each expected posterior cerebral artery territory, and over the anterior circulation territories. Two grade values are obtained for vertebral artery disruptions. The first is the cerebellar grade, determined by the ratio of cerebellar counts to those anterior circulation counts, and the second is the posterior cerebral artery grade, determined by the ratio of posterior cerebral artery counts to anterior circulation counts, on a scale summarized in Table 2B. The overall grade is whichever ratio gives the higher grade. The categories for radionuclide numeric grades of disruption were determined by comparing the visual and numeric radionuclide grades on 20 consecutive postdisruption scans performed before this study. Regions of interest are drawn to avoid areas of tumor or major venous structures.

TABLE 2A: Grading systems for anterior circulation disruptions

	CT and Radionuclide Visual Activity	CT Quantitative	RN Quantitative
0 (Nil)	None	<0	<1.19
1 (Moderate)	Barely seen	0–5	1.19–1.40
2 (Good)	Easily seen	5–25	1.40–1.62
3 (Excellent)	Marked	>25	>1.62

Note.—Visual grades are based on the difference between enhancement or activity between the disrupted and nondisrupted territories. CT quantitative grades are based on HU differences between the disrupted and nondisrupted middle cerebral artery territories. Radionuclide quantitative grades are based on count ratios between regions of interest in the disrupted and nondisrupted ICA territories.

Clinical Utility of Grading Disruption

When the first disruption is performed in the internal carotid artery, the flow rate of mannitol is determined by using a test injection of contrast so there is a reflux into the ipsilateral external carotid artery. For vertebral artery disruptions, the initial flow rate for mannitol is determined using a test injection of contrast so there is reflux into the contralateral vertebral artery. Initial flow rates are based on laboratory studies, which show that infusing 25% mannitol for 30 seconds in the internal carotid or vertebral arteries was the minimum osmolality and infusion time to obtain a blood-brain barrier disruption (8, 9). Animal studies have shown a dependence of the degree of disruption on the flow rate of mannitol (10). Based on these laboratory data the results of imaging studies are used to influence the

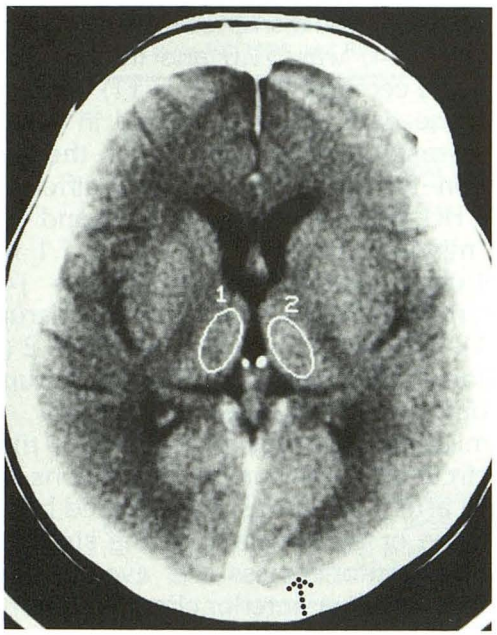

A

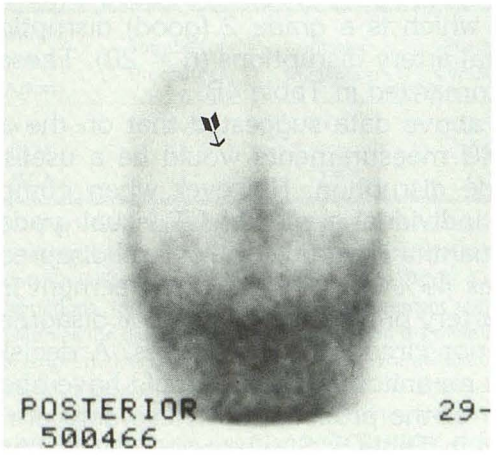

B

Fig. 4. *A*, CT scan of patient 5 after a blood-brain barrier disruption in the left vertebral artery shows evidence of a grade 1 (moderate) disruption (*arrow*). *Ellipses* are examples of regions of interest in the right (*1*) and left (*2*) thalami.

B, Posterior view of a radionuclide scan in the same patient on the same date shows an example of a grade 1 (moderate) disruption in the thalami and posterior cerebral artery territories (*arrow*).

mannitol flow rates based on the following rationale: If a nil or moderate disruption is obtained the flow rate of mannitol is increased by 1 cc/sec the next time a disruption is performed in that vessel. If a good or excellent disruption is obtained the flow rate of mannitol is not changed.

Comparison of Grading Systems

Each disruption had four grades: a CT visual grade, a radionuclide visual grade, a CT quantitative grade, and a radionuclide quantitative grade. To evaluate the different grading systems three sets of comparisons were made, comparing CT visual grading with radionuclide visual grading, CT visual grading with CT quantitative grading, and radionuclide visual grading with radionuclide quantitative grading. The comparisons between grading systems were divided into areas of comparison for: 1) all disruptions, 2) posterior circulation disruptions, and 3) anterior circulation disruptions. Square graphs were then analyzed for the percentage of procedures in which there was either disagreement between grading systems or a decision to change the mannitol flow rate.

Results

There were only two seizures in 45 procedures for a rate of 4%. There was one episode of prolonged obtundation and one deep venous thrombosis. These were the only complications.

When comparing visual CT and visual radionuclide grading there was a 16% overall disagreement rate, a 25% disagreement in vertebral artery disruptions, and an 8% disagreement in anterior circulation disruptions. Disagreements would result in a decision to change the mannitol flow rate in 9% of the procedures. These data are summarized in Table 3.

Quantitative CT data showed the medians of HU measurements to vary from 40.3 to 55.4 with narrow interquartile ranges. In anterior circulation procedures HU in the middle cerebral artery territory was used to measure disruptions. The me-

TABLE 2B: Grading systems for posterior circulation disruptions

	CT and Radionuclide Visual Activity	CT Quantitative	Radionuclide Cerebellar Quantitative	Radionuclide Posterior Cerebral Artery Quantitative
0 (Nil)	None	<2.5	<1.14	<1.58
1 (Moderate)	Barely	2.5–7.5	1.14–1.49	1.58–2.05
2 (Good)	Easily	7.5–12.5	1.49–1.85	2.05–2.53
3 (Excellent)	Marked	>12.5	>1.85	>2.53

Note.—CT and radionuclide visual grades are based on the difference between enhancement and activity between the disrupted and nondisrupted territories. CT grades are based on the differences between the average HU in six posterior circulation territories (bilateral cerebellar hemispheres, bilateral thalami, and bilateral posterior cerebral artery) less the average HU in the four anterior circulation territories (bilateral anterior cerebral artery and middle cerebral artery). The radionuclide cerebellar grade is based on the count ratio of the cerebellum to the anterior cerebral artery and middle cerebral artery territories. The radionuclide posterior cerebral artery grade is based on the count ratio of the posterior cerebral artery territories to the anterior cerebral artery and middle cerebral artery territories.

TABLE 3: Square-plot comparison of visual grades: CT versus radionuclide scanning

A. All

CT Grade	RN Grade 0	1	2	3	Total
0	4	1	0	0	5
1	0	5	1	0	6
2	0	2	20	1	23
3	0	1	1	9	11
Total	4	9	22	10	45

Disagreement = 16%, change in mannitol flow rate = 9%

B. Vertebral artery

CT Grade	RN Grade 0	1	2	3	Total
0	1	1	0	0	2
1	0	3	0	0	3
2	0	1	5	1	7
3	0	1	1	6	8
Total	1	6	6	7	20

Disagreement = 25%, change in mannitol flow rate = 10%

C. Anterior circulation

CT Grade	RN Visual 0	1	2	3	Total
0	3	0	0	0	3
1	0	2	1	0	3
2	0	1	15	0	16
3	0	0	0	3	3
Total	3	3	16	3	25

Disagreement = 8%, change in mannitol flow rate = 8%

Note.—CT grades are plotted on the vertical axis and radionuclide grades on the horizontal axis. The grading systems are summarized in Table 2. For Tables 3, 5 and 6, the diagonals highlighted show the procedures in which both grading systems agreed. The four upper right and four lower left squares in each matrix are procedures in which a decision to change the mannitol flow rate would occur based on disagreements between grading systems.

dian HU value in the disrupted left middle cerebral artery (n = 14) was 51.0 and in the disrupted right middle cerebral artery (n = 11) territory was 49.0. These data are summarized in Table 4A. Group measures of disruption for the anterior circulation territories showed the difference in median HU between the disrupted and nondisrupted middle cerebral artery to be 7.1 for left internal carotid artery disruptions (n = 14) and 7.5 for right middle cerebral artery disruptions (n = 11). This would translate to grade 2 (good) disruptions for anterior circulation disruptions. These data are summarized in Table 4B.

A similar analysis was performed for the posterior circulation territories. Disruptions in the vertebral artery territories were graded by taking the average of the medians of the six posterior circulation territories less the averages of the medians for the four anterior circulation territories to obtain a grade of disruption of the entire group of procedures. This calculation gave a number of 10.90, which is a grade 2 (good) disruption for vertebral artery disruptions (n = 20). These data are summarized in Table 4B.

The above data suggested that on the aggregate, HU measurements would be a useful way to grade disruption. However when comparing the 45 individual grades of CT visual grade with a CT quantitative grade, the overall disagreement rate was 49% with a 40% disagreement in vertebral artery procedures and a 56% disagreement in anterior circulation procedures. A decision to change mannitol flow rates would have occurred in 16% of the procedures. These data are summarized in Table 5. Similar results were obtained comparing radionuclide visual and quantitative grading systems with a disagreement rate of 44% overall, a 35% disagreement in vertebral artery disruptions, and a 56% disagreement in anterior circulation disruption. Discrepancies between grading systems would have resulted in a decision to alter the mannitol flow rate in 22% of the procedures. These data are summarized in Table 6.

Discussion

The blood-brain barrier serves to protect the brain from toxins. Substances that are well tolerated systemically are often toxic when given in conjunction with osmotic blood-brain barrier disruption (6, 10–12). Prior studies have shown a lower incidence of nonneurologic side effects when nonionic rather than ionic contrast agents are given intravenously for enhanced CT scan-

TABLE 4A: Median and interquartile ranges for the HU measurements taken in varying regions of interest for VA, LICA, and RICA disruptions

Region of Interest	VA (20 Disruptions)		LICA (14 Disruptions)		RICA (11 Disruptions)	
	Median	IQR	Median	IQR	Median	IQR
RACA	42.9	6.4	45.4	6.1	42.3	5.1
LACA	41.3	5.1	46.8	6.9	41.3	2.9
RMCA	41.4	4.3	43.9	6.6	49.0	8.4
LMCA	41.4	4.0	51.0	5.3	41.5	3.6
RPCA	50.0	10.9	45.0	2.8	43.3	7.4
LPCA	52.3	8.5	46.1	6.0	42.8	10.4
Right cerebellum	55.4	6.0	49.8	6.4	47.6	7.8
Left cerebellum	55.3	7.5	50.1	5.7	48.0	4.9
Right thalamus	50.6	6.2	42.2	4.7	42.2	3.5
Left thalamus	52.2	8.7	43.1	4.4	40.3	5.0

Note.—All units are in HU. Interquartile range (IQR) is the range between the lowest and highest quartile (ie, the middle 50% of values) of these distributions of HU measurements taken in regions of interest. LACA indicates left anterior cerebral artery; LICA, left internal carotid artery; LMCA, left middle cerebral artery; LPCA, left posterior cerebral artery; RACA, right anterior cerebral artery; RICA, right internal carotid artery; RMCA, right middle cerebral artery; RPCA, right posterior cerebral artery; and VA, vertebral artery.

TABLE 4B: CT quantitative measure of disruption

Mannitol-Infused Artery	Number of Procedures	Anterior Circulation	Posterior Circulation
VA	20	0	10.90
LICA	14	7.1	0.94
RICA	11	7.5	0.73

Note.—For anterior circulations measurements the number calculated was the difference between median (HU) measurements of disrupted and nondisrupted middle cerebral artery territories (see Fig 2). For vertebral artery disruptions, the anterior circulation measurement number in the above table was the difference between the median HU measurements of the left and right middle cerebral artery territories. The posterior circulation measurement of disruption was the average of the medians of the six posterior circulation territories less the average of the medians of the four anterior circulation territories (see Figs 1–4). This table shows that the median of the distribution of HU predicted a good (grade 2) disruption with the appropriate vascular territories for these groups of procedures.

ning or intraarterially with cerebral angiography (13–27). Metaanalyses of many studies have suggested that there is no difference in neurologic complications between ionic and nonionic contrast media when the agents are given intravascularly (28). Administering contrast media intravenously in conjunction with osmotic blood-brain barrier disruption results in a 10-fold increase in drug delivery to the brain (29). A prior study showed a 16% incidence of seizures, a major manifestation of neurologic toxicity when meglumine iothalamate, an ionic iodine-based contrast medium, was injected intravenously in conjunction with osmotic blood-brain barrier disruption (5). This study showed only a 4% rate of seizures when an equivalent amount of iodine was injected using a nonionic contrast medium. This suggests less neurologic toxicity for nonionic contrast media and may be relevant to the choice of intravascular contrast media when imaging a patient who may have a compromised blood-brain barrier.

There was good concordance between the CT and radionuclide visual grades. Very little change in mannitol flow rate would occur if only CT scanning or radionuclide scanning was used to image disruption. This is similar to prior animal studies which have shown visual grading of disruption on CT scans to correspond well with Evans blue albumin staining (4). Most of the discrepancies, when comparing CT and radionuclide visual grading systems, were in vertebral artery disruptions. These disagreements also may be caused by artifact in the posterior fossa on CT scans. CT scanning is the preferred method to image disruption because of the superior spatial resolution.

Marked disagreements occurred when comparing both CT visual and numeric grading as well as radionuclide visual and numeric grading. There are a few possible reasons for this result. When quantitative evaluation of radionuclide scans in the posterior circulation territories was performed, separate grades were obtained for the supratentorial and infratentorial posterior circulation territories. This would correct for discrepancies that occur when grading disruption caused by fetal origins of the posterior cerebral artery, an anatomic variation that may occur in about 15% of patients (30, 31). When using CT and radionuclide scanning to evaluate anterior circulation disruptions, the middle cerebral artery ter-

TABLE 5: Square plot of CT quantitative grade versus comparison of visual

A. All disruptions

CT Visual \ CT Quantitative	0	1	2	3	Total
0	3	2	0	0	5
1	1	1	3	1	6
2	1	2	10	10	23
3	0	0	2	9	11
Total	5	5	15	20	45

Disagreement = 49%, change in mannitol flow rate = 16%

B. Vertebral artery

CT Visual \ CT Quantitative	0	1	2	3	Total
0	1	1	0	0	2
1	1	1	1	0	3
2	0	2	4	1	7
3	0	0	2	6	8
Total	2	4	7	7	20

Disagreement = 40%, change in mannitol flow rate = 15%

C. Anterior circulation

CT Visual \ CT Quantitative	0	1	2	3	Total
0	2	1	0	0	3
1	0	0	2	1	3
2	1	0	6	9	16
3	0	0	0	3	3
Total	3	1	8	13	25

Disagreement = 56%, change in mannitol flow rate = 16%

Note.—CT visual grade is plotted on the vertical axis; CT numerical grade is plotted on the horizontal axis. The grading systems are summarized in Table 2.

TABLE 6: Square plot comparison of quantitative radionuclide grades versus visual radionuclide grades of disruption

A. All procedures

RN Visual \ RN Quantitative	0	1	2	3	Total
0	3	1	0	0	4
1	0	5	2	2	9
2	0	4	10	8	22
3	0	2	1	7	10
Total	3	12	13	17	45

Disagreement = 44%, change in mannitol flow rate = 22%.

B. Vertebral artery

RN Visual \ RN Quantitative	0	1	2	3	Total
0	1	0	0	0	1
1	0	4	1	1	6
2	0	2	3	1	6
3	0	1	1	5	7
Total	1	7	5	7	20

Disagreement = 35%, change in mannitol flow rate = 25%

C. Anterior circulation

RN Visual \ RN Quantitative	0	1	2	3	Total
0	2	1	0	0	3
1	0	1	1	1	3
2	0	2	7	7	16
3	0	1	0	2	3
Total	2	5	8	10	25

Disagreement = 52%, change in mannitol flow rate = 20%

Note.—Visual radionuclide grades are plotted on the vertical axis and numerical on the horizontal axis. The grading systems are summarized in Table 2.

ritories were used; the middle cerebral artery territories are almost always supplied by the internal carotid arteries. Regions of interest on both radionuclide and CT scans were drawn to exclude areas of the brain that showed enhancement caused by vascular structures or by tumor. The HU measurements shown in Table 4 indicated these data could be used to predict disruption in a large number of procedures. However, when comparing visual and quantitative CT grades in Table 5 and visual and quantitative radionuclide grades in Table 6 there were striking disagreements. Quantitative analysis of the scan was not useful in predicting the degree of disruption in an individual patient.

Despite allowing for variations in the circle of Willis, drawing representative regions of interest, and using sophisticated statistical analysis, quantitative interpretation of neuroimaging studies did not add useful data to the interpretation of the neuroradiologist. Using grading of a disruption as a paradigm, it seems that the cognitive and visual skills of a neuroradiologist are necessary to interpret neuroimaging studies; quantitative methods do not add clinically relevant information. An editorial on positron emission tomography scanning showed a similar conclusion in that quantitative analysis of images did not add to the diagnostic yield from visual interpretation of images (32). This analysis may be relevant to other imaging systems in which advances in technology do not improve patient outcomes (33, 34).

Conclusion

Nonionic iodine-based contrast media, when administered intravenously in conjunction with osmotic blood-brain barrier disruption, show a lower incidence of seizures than ionic contrast media. CT scanning enhanced with nonionic contrast is the preferred method to image disruption caused by superior spatial resolution. Visual analysis of the scans seems to be superior to quantitative analysis when imaging disruption.

Acknowledgments

Our thanks to Patricia Butler for her editorial assistance.

References

1. Neuwelt EA, Frenkel EP, Gumerlock MK, Braziel R, Dana B, Hill SA. Developments in the diagnosis and treatment of primary CNS lymphoma: a prospective series. *Cancer* 1986;58:1609–1620
2. Neuwelt EA, Howieson J, Frenkel EP, et al. Therapeutic efficacy of multiagent chemotherapy with drug delivery enhancement by blood-brain barrier modification in glioblastoma. *Neurosurgery* 1986;19:573–582
3. Neuwelt EA, Goldman D, Dahlborg SA, et al. Primary CNS lymphoma treated with osmotic blood-brain barrier disruption: prolonged survival and preservation of cognitive function. *J Clin Oncol* 1991;9: 1580–1590
4. Neuwelt EA, Maravilla KR, Frenkel EP, Barnett P, Hill S, Moore RJ. Use of enhanced computerized tomography to evaluate osmotic blood-brain barrier disruption. *Neurosurgery* 1980;6:49–56
5. Neuwelt EA, Specht HD, Howieson J, et al. Osmotic blood-brain barrier modification: Clinical documentation by enhanced CT scanning and/or radionuclide brain scanning. *AJNR Am J Neuroradiol* 1983;4:907–913
6. Roman-Goldstein SM, Barnett PA, McCormick CI, Ball MJ, Ramsey F, Neuwelt EA. Effect of gadopentetate dimeglumine administration after osmotic blood-brain barrier disruption: toxicity and MR imaging findings. *AJNR Am J Neuroradiol* 1991;12:885–890
7. Runge VM, Price AC, Wehr CJ, Atkinson JB, Tweedle MF. Contrast enhanced MRI: evaluation of a canine model of osmotic blood-brain barrier disruption. *Invest Radiol* 1985;20:830–844
8. Neuwelt EA, Barnett PA. Blood-brain barrier disruption in the treatment of brain tumors. Animal studies. In: Neuwelt EA, ed. *Implications of the blood-brain barrier and its manipulation. Vol 1. Clinical aspects.* New York: Plenum, 1989:107–193
9. Rapoport SI, Fredericks WR, Ohno K, Pettigrew KD. Quantitative aspects of reversible osmotic opening of the blood-brain barrier. *Am J Physiol* 1980;238:R421–R431
10. Neuwelt EA, Glasberg M, Diehl J, Frenkel EP, Barnett P. Osmotic blood-brain barrier disruption in posterior fossa of the dog. *J Neurosurg* 1981;55:742–748
11. Neuwelt EA, Glasberg M, Frenkel E, Barnett P. Neurotoxicity of chemotherapeutic agents after blood-brain barrier modification: neuropathological studies. *Ann Neurol* 1983;14:316–324
12. Neuwelt EA, Pagel M, Barnett P, Glasberg M, Frenkel EP. Pharmacology and toxicity of intracarotid adriamycin administration following osmotic blood-brain barrier modification. *Cancer Res* 1981;41:4466–4470
13. Ahlgren P. Iohexol compared to urografin meglumine in cerebral angiography. A randomized, double blind, cross-over study. *Neuroradiology* 1982;23:195–198
14. Bird CR, Drayer BP, Velaj R, et al. Safety of contrast media in cerebral angiography: iopamidol versus methylglucamine iothalamate. *AJNR Am J Neuroradiol* 1984;5:801–803
15. Bryan RN, Miller SL, Roehm JOF, Weatherall PT. Neuroangiography with iohexol. *AJNR Am J Neuroradiol* 1983;4:344–346
16. Caro JJ, Trindade E, McGregor M. The risks of death and of severe nonfatal reactions with high- vs low-osmolality contrast media: a meta-analysis. *AJR Am J Roentgenol* 1991;156:825–832
17. Hindmarsh T, Bergstrand G, Ericson K, Olivecrona H. Comparative double-blind investigation of meglumine metrizoate, metrizamide, and iohexol in carotid angiography. *AJNR Am J Neuroradiol* 1983;4: 347–349
18. Holtas S, Cronqvist S, Renaa T. Contrast enhanced brain CT comparison between iohexol and metrizoate. *Invest Radiol* 1985;20: S62–S64
19. Katayama H, Yamaguchi K, Kozuka T, Takashima T, Seez P, Matsuura K. Adverse reactions to ionic and nonionic contrast media: a report from the Japanese committee on safety of contrast media. *Radiology* 1990;175:621–628
20. Kido DK, Potts DG, Bryan RN, et al. Iohexol cerebral angiography. Multicenter clinical trial. *Invest Radiol* 1985;20:S55–S57
21. Molyneux AJ, Sheldon PWE. A randomized blind trial of iopamidol and meglumine calcium metrizoate (triosil 280, isopaque cerebral) in cerebral angiography. *Br J Radiol* 1982;55:117–119

22. Nakstad P, Sortland O, Aaserud O, Lundervold A. Cerebral angiography with the non-ionic water-soluble contrast medium iohexol and meglumine-Ca-metrizoate. *Neuroradiology* 1982;23:199–202
23. Pelz D, Fox AJ, Vinuela F. Clinical trial of iohexol versus conray 60 for cerebral angiography. *AJNR Am J Neuroradiol* 1984;5:565–568
24. Ramsey RG, Czervionke L, Dommers M, James ME, Huckman MS, Russel EJ. Safety and efficacy of sodium and meglumine ioxaglate (hexabrix) and hypaque M60%® in contrast-enhanced computed cranial tomographic scanning. A double-blind clinical study. *Invest Radiol* 1987;22:56–61
25. Skalpe IO, Anke IM. Complications in cerebral angiography. A comparison between the nonionic contrast medium iohexol and meglumine metrizoate (isopaque cerebral). *Neuroradiology* 1983;25: 157–160
26. Skalpe IO, Hordvik. Comparison of side effects during cerebral computed tomograph with a nonionic (iohexol) and an ionic (metrizoate) contrast medium. *AJNR Am J Neuroradiol* 1983;4:326–328
27. Wolf GL, Arenson RL, Cross AP. A prospective trial of ionic vs nonionic contrast agents in routine clinical practice: comparison of adverse effects. *AJR Am J Roentgenol* 1989;152:838–844
28. Kinnison ML, Powe NR, Steinberg EP. Results of randomized controlled trials of low- versus high-osmolality contrast media. *Radiology* 1989;170:381–389
29. Neuwelt EA, Frenkel E, D'Agostino AN, et al. Growth of human lung tumor in the brain of the nude rat as a model to evaluate antitumor agent delivery across the blood-brain barrier. *Cancer Res* 1985;45:2827–2833
30. Osborn AG, Maack JG. *Introduction to cerebral angiography*. Philadelphia: Harper & Row, 1980:143–165
31. Wollschlaeger G, Wollschlaeger PB. The circle of willis. In: Newton TH, Potts DG, eds. *Radiology of the skull and brain angiography*. St Louis: Mosby, 1974:1171–1201
32. DiChiro G, Brooks RA. PET quantitation: blessing and curse. *J Nucl Med* 1988;29:1603–1604
33. Bucci VA, Health outcomes research: its influence on clinical decision making and the development of new imaging technologies. *AJNR Am J Neuroradiol* 1991;12:397–399
34. Huckman MS. Outcomes: where the rockets come down. *AJNR Am J Neuroradiol* 1991;12:400–401